Biointerface Research in Applied Chemistry
Open-Access Journal (ISSN: 2069-5837)

Article
Volume 13, Issue 5, 2023, 472
https://doi.org/10.33263/BRIAC135.472

Electrochemical Studies of *Erica arborea* Extract as a Green Corrosion Inhibitor for C-steel in Sulfuric Acid Medium

Mohamed S. Almahdy [1], Ahmed F. Molouk [1], Ahmed El-Hossiany [1,2], Abd El-Aziz S. Fouda [1,*]

[1] Department of Chemistry, Faculty of Science, El-Mansoura University, Egypt; asfouda@mans.edu.eg (A.S.F.);
[2] Delta Fertilizers Company on Talkha, Egypt; dr.ahmedselm@gmail.com (A.-H.);
* Correspondence: asfouda@hotmail.com (A..S.F.);

Scopus Author ID 56231506400

Received: 14.07.2022; Accepted: 30.08.2022; Published: 27.12.2022

Abstract: The carbon steel (CS) corrosion inhibition in H_2SO_4 media by *Erica arborea* leaves (EA) extract as a sustainable green inhibitor was described here. The mass loss technique (ML), potentiodynamic polarization (PDP), electrochemical frequency modulation (EFM), and electrochemical impedance spectroscopy were all used in this investigation (EIS). In addition, Atomic Force Microscopy was also used to examine the metal surface morphology (AFM). The EIS demonstrated that the *Erica arborea* extract generated a thin protective coating on the metal surface and that utilizing 1000 ppm of *Erica arborea* extract allows for 93.4 % corrosion inhibition effectiveness (CIE). According to the PDP curves, the *Erica arborea* extracts act as a mixed-type inhibitor. It was discovered that the inhibition efficiency increased as the *Erica arborea* extract dosages increased. The system's kinetic characteristics and thermodynamic adsorption have also been measured and investigated. The results collected demonstrated that *Erica arborea* adsorption on metal surfaces followed the Langmuir isotherm and that the *Erica arborea* extract operates via physisorption according to the activation energy (E_a^*). The findings of disparate measurements were in good agreement.

Keywords: corrosion inhibition; carbon steel; hydrochloric acid; potentiodynamic polarization; electrochemical impedance spectroscopy; electrochemical frequency modulation; atomic force microscopy; activation energy.

1. Introduction

The study of the corrosion of metals and how to preserve them from corrosion is critical owing to the difficulties it causes, such as economic losses resulting from material degradation. Corrosion is defined as the corrosion and disintegration of metals and alloys caused by chemical and electrochemical interactions with their surroundings [1]. Because of its perfect mechanical properties at elevated temperatures, ease of fabrication, and low cost, CS is one of the most widely used materials in petroleum, pipelines, tanks, vessels, equipment, automobile body components, structural shapes (I-beams, channel, and angle iron), construction, bridge components, food cans, and other industries. However, it corrodes when in contact with acidic solutions, so scientific researchers are working hard to overcome this problem.

Plant Extract Preparation: Acidic solutions are employed in industrial applications, with sulfuric acid being the most commonly used to eliminate oxides generated in carbon steel and oil refineries by chemical methods [2-5]. As a result, current research focuses on nonhazardous, biodegradable, less expensive, and ecologically friendly corrosion inhibitors. Plant extracts represent a plenteous category of corrosion inhibitors as most of these materials are easily obtainable and non-poisonous [6-7]. Many studies examining plant extracts have revealed that various leaf, root, bark, stem, pulp, and fruit extracts are being investigated as corrosion inhibitors for various metals and alloys [8]. Plant extracts such as *olives leaf* [9], *Jathropa leaf* [10], *Inula viscosa* [11], *Malpighia glabra leaf* [12], *Oxalis stricta leaf* [13], *Soybean* [14], *Terminalia arjuna leaves* [15] among others have been investigated as good corrosion inhibitors. In this study, EA extracts were utilized to inhibit CS corrosion in 0.5M H_2SO_4. Different tests are utilized to study the inhibition efficiency of EA. In ML and electrochemical techniques, the corrosion rate increases when EA extract concentration increases. Metal's surface is premeditated by AFM, and XPS.

2. Materials and Methods

2.1. Composition of CS sample.

Table 1 lists the chemical components found in the CS sample.

Table 1. The wt. % of CS pieces was given.

wt%	C	Si	Mn	P	Fe
CS	0.17-0.2	0.003	0.35	0.025	the rest

2.2. Chemicals.

2.2.1. Inhibitor.

i. Preparation of plant extract.

Soxhlet extraction was done on powdered *Erica arborea* leaf samples using 96% ethanol for 6 hours, according to the established Soxhlet technique. The extracted extracts were then filtered and evaporated at 40 °C under reduced pressure until dry. The dried extracts were kept at 4 °C, away from light, until they were analyzed. The examined extract was liquefied in ethanol (2g/L) and stored in a refrigerator [16]. Figure 1 shows that the CA extract contains 72 different polyphenol compounds from various subclasses (phenolic acids and derivatives; flavan-3-ols and proanthocyanidins; flavonoid glycosides; flavonoid aglycones), with a high content of palmitic acid, 9, 12, 15-Octadecatrien-1-ol, (Z,Z,Z)- and nonacosane [17]. We create different concentrations of EA extract using the solution (2000 ppm) (300, 450, 600, 750, 850, and 1000 ppm).

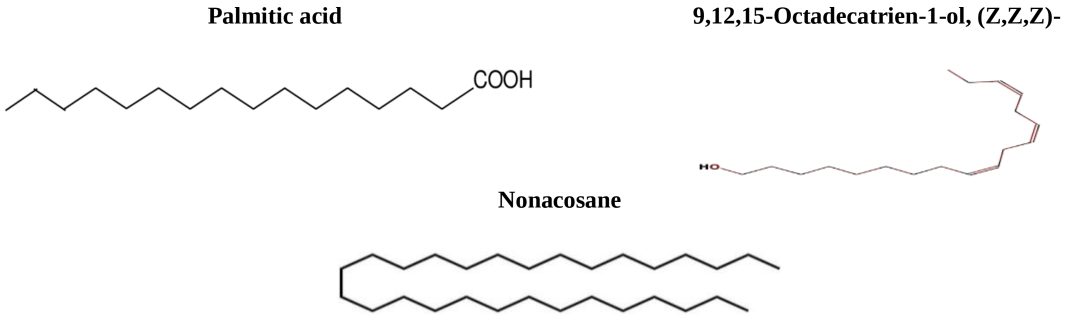
Palmitic acid

9,12,15-Octadecatrien-1-ol, (Z,Z,Z)-

Nonacosane

Figure 1. Chemical markers of CA.

2.2.2. Solutions.

The corrosive medium used in the experiments was 0.5 M H_2SO_4, which was made from analytical reagent grade H_2SO_4 and distilled water.

2.3. Techniques used to compute inhibition efficiency.

2.3.1. Mass loss method (ML).

The WL methodology is a straightforward method for calculating the inhibitory effects of EA extract on CS in 0.5M H_2SO_4. This approach employed square pieces of CS measuring (2 cm x 2 cm x 0.2 cm). The C-S pieces were produced by using emery sheets with different degrees (600, 1000, 1200, 2000) and then removing contaminants from the surface with acetone. The inhibition of CS corrosion was studied at various temperatures (25, 30, 40, 50) and concentrations of EA extract solution (300, 450, 600, 750, 850, and 1000 ppm). We may determine corrosion rate (CR), surface covering area (θ), and inhibition efficiency (% IE) using the following eqn. [18].

$$\% \text{ IE} = \theta \times 100 = [1 - (W/W^o)] \times 100 \qquad (1)$$

where W^o, and W are the MR, presence, and absence, respectively, a different concentration of examined inhibitor is continuously added.

2.3.2. Electrochemical methods.

The %IE in electrochemical methods is computed using three methods: PP, EIS, and EFM. Three different electrodes are placed in a glass cell for electrochemical research. Reference electrode of Ag/AgCl(s), an auxiliary electrode of platinum wire, and a CS working electrode with 1 cm^2 outer area. The working electrode's surface must be mechanically prepared in the same manner as stated previously. The operating electrode was a polisher with a paper grit of 1200. Before the experiments, the electrode was immersed in H_2SO_4 at a natural potential for half an hour until it reached a steady state. The CS electrode was submerged in the solution for 20 minutes after being prepared to establish a steady state, i.e., open circuit potential (OCP). Gamry Instrument (PCI4/750) Potentiostat/Galvanostat/ZRA was used for all electrochemical experiments.

i. PP method.

Tafel curves were generated using this approach with a scan rate of 1mVs^{-1}. All experiments were carried out in freshly prepared solutions at 25 °C. We can determine %IE and [19] from the result data.

$$\text{IE } \% = 100 \times \theta = 100 \times [1- (i_{corr(inh)} / i_{corr(free)})] \qquad (2)$$

$i_{corr(inh)}$ and $i_{corr(free)}$ are the corrosion currents in the presence and absence of extract, respectively.

ii. EIS technique.

EIS experiments were performed at OCP using AC signals of 5 mV in the frequency range (0.2Hz to 100 kHz). The diameters of the capacitive loops improve in the presence of inhibitors, and are lead to the capacitive of the amount of process corrosion inhibition, in reverse to the lower of the C_{dl}, which is supplied:

$$C_{dl} = 1/ (2 \pi f_{max} R_p) \qquad (3)$$

f_{max} = frequency maximum. The %IE and (θ) given from EIS analyses were acquired through the following relation:

$$IE\ \% = 100 \text{ x } \theta = 100 \times [1- (R^{\circ}_{p}/R_{p})] \quad (4)$$

R^{o}_{p} and R_p are the charge resistance in the presence and absence of extract, respectively.

iii. EFM technique.

The EFM investigation was performed using a signal of 10 mV amplitude and two single waves of 2 and 5 Hz [20]. The bigger peaks were used to calculate the causality factors (CF-2 and CF-3), (β_c and β_a), and (i_{corr}) [21]. The inhibition efficiencies of % IE EFM were computed as follows:

$$\%IE_{\ EFM} = 100 \text{ X } [1- (i_{corr.} /i^{o}_{corr.})] \quad (5)$$

where i^{o}_{corr} and i_{corr} are current corrosion in the presence and absence of EA extract respectively.

2.4. Surface analysis.

i. Atomic force microscopy.

AFM spectroscopy produces a three-dimensional picture of the film produced on the surface of the metal. This was accomplished using Thermo Fisher Nicolet IS10, USA, with a spectral range of 400 – 4000 cm^{-1}. The picture has a roughness, which indicates the inhibitor response.

ii. X-ray photoelectron spectroscopy analysis (XPS).

XPS K-ALPHA was used to describe the surface of CS after it was immersed in 0.5M H_2SO_4 solution in the absence and presence of 1000 ppm EA for 12 hours (Themo Fisher Scientific, USA).

3. Results and Discussion

3.1. Mass loss (ML) tests.

The ML-time curves were measured in the presence and absence of different concentrations of EA extract, as shown in Figure 2. Table 2 shows the CR, IE, θ, and % IE values (2). According to the table, CR decreases when EA extract concentrations increases due to increases in the adsorption of EA extract on the CS surface. The %IE increases with increasing EA extract concentrations and temperature [22].

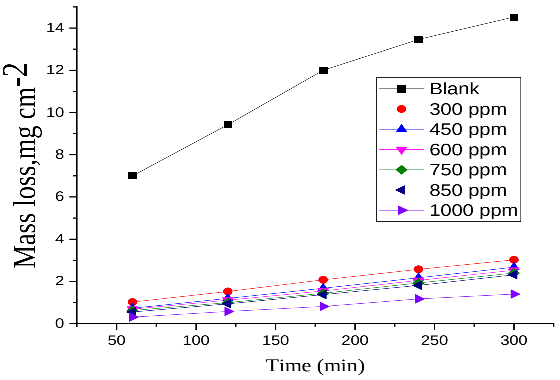

Figure 2. Curves of mass loss *vs.* time of the CS corrosion in 0.5M H_2SO_4 in the presence and absence of different concentrations of EA extract at 25°C.

Table 2. ML measurements for CS at temperatures (25-50) at 180 min in the presence and absence of different concentrations of EA extract.

Temp. (ºC)	[inh], ppm	CR (mg cm^{-2} min^{-1})	ϴ	% IE
25	Blank	0.0667	--	--
	300	0.0115	0.827	82.7
	450	0.0093	0.860	86.0
	600	0.0086	0.871	87.1
	750	0.0080	0.880	88.0
	850	0.0076	0.885	88.5
	1000	0.0045	0.933	93.3
30	Blank	0.0700	--	--
	300	0.0132	0.812	81.2
	450	0.0097	0.861	86.1
	600	0.0094	0.866	86.6
	750	0.0083	0.881	88.1
	850	0.0080	0.886	88.6
	1000	0.0072	0.897	89.7
40	Blank	0.1032	--	--
	300	0.0251	0.757	75.7
	450	0.0231	0.776	77.6
	600	0.0209	0.797	79.7
	750	0.0204	0.802	80.2
	850	0.0194	0.812	81.2
	1000	0.0193	0.813	81.3
50	Blank	0.1778	--	--
	300	0.0558	0.686	68.6
	450	0.0535	0.699	69.9
	600	0.0525	0.705	70.5
	750	0.0509	0.714	71.4
	850	0.0501	0.718	71.8
	1000	0.0489	0.725	72.5

3.1.1. Adsorption isotherms.

Adsorption isotherms provide information on the interaction between EA extract and the CS surface in 0.5M H_2SO_4. Adsorption isotherms include the Langmuir, Temkin, Freundlich, Bockris-Swinkles, and Flory-Huggins isotherms [23]. The Langmuir adsorption isotherm was discovered to offer the greatest information about the interaction between the adsorbed layers of the EA extract and the surface of CS in 0.5M H_2SO_4, as illustrated by (Eq. 6). The connection between (C) and C/ is linear, as shown by straight lines (Figure 3). As shown in (Eq. 7) [24],

$$C/ϴ = 1/K_{ads} + C \qquad (6)$$

K_{ads} belongs to ΔG^0_{ads}:

$$\Delta G^0_{ads} = RT \ln (K_{ads} \text{ x } 55.5) \qquad (7)$$

where K_{ads}=constant equilibrium, R=Universal gas constant, T=temperature in Kelvin and C=EA extract conc.

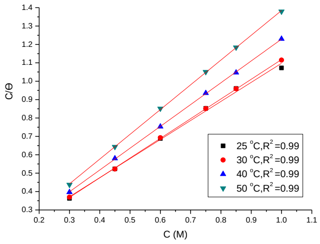

Figure 3. Plot of Langmuir adsorption of CS in 0.5M H_2SO_4 in the presence and absence of different concentrations of EA extract.

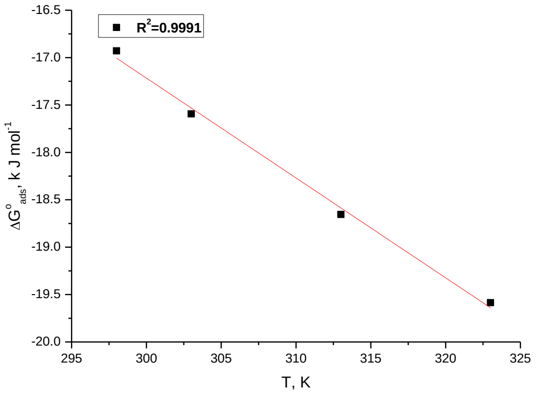

Figure 4. Plot of log K_{ads} vs. 1/T for the adsorption of EA extract on CS in 0.5M H_2SO_4 at (25-50^{0}C).

Table 3. Adsorption parameters of EA extract on CS surface by Langmuir isotherm at (25-45^{0}C)

Compound	Temp K	k_{ads}x10^{-3} M^{-1}	$-\Delta G^{\circ}_{ads}$ kJ mol^{-1}	$-\Delta H^{\circ}_{ads}$ kJ mol^{-1}	$-\Delta S^{\circ}_{ads}$ J mol^{-1} K^{-1}
EA	298	16	16.8	13.3	102
	303	21	17.6		
	313	23	18.6		
	323	26	19.5		

According to the statistics in Table 3:

1. K_{ads} values increase when temperature increases.

2. ΔG^{o}_{ads} -ve sign indicates that the EA extract is adsorbed spontaneously on CS surface and the stabiliry of the adsorbed layer [25].

3. ΔG^{o}_{ads} data more than 20 kJ mol^{-1}, which is given physisorption and spontaneous.

The enthalpy(ΔH°_{ads}) **and entropy (ΔS^{o}ads) of adsorption can be assessed using the following Eqs.:**

$\ln K_{ads} = -\Delta H^{o}_{ads}/RT$ + constant (Figure 4) (8)

$\Delta G^{\circ}_{ads} = \Delta H^{o}_{ads} - -\Delta S^{\circ}_{ads}$ **(9)**

4. ΔH^{o}_{ads} -ve sign indicate that the EA extract adsorption is an exothermic process.

5. ΔS^{o}_{ads} has a -ve sign because EA molecules that were freely flowing in the bulk solution were ordered adsorbed onto CS, resulting in a reduction in entropy" [26].

3.1.2. Thermodynamic corrosion parameter.

The activation parameters of the CS corrosion in 0.5 M H_2SO_4 in the presence and absence of various doses of EA extract are obtained from Arrhenius and transition state equations (Eq. 10,11)

$$k_{corr} = A\ e^{-E^*a/RT} \tag{10}$$

$$k_{corr} = RT/Nh\ e^{(\Delta S^*/R)}\ e^{(-\Delta H^*/RT)} \tag{11}$$

E^*_a = activation energy, As illustrated in Figure 5, we plot log k_{corr} *versus* 1/T for CS in 0.5M H_2SO_4 in the presence and absence of different concentrations of EA extract than from the slope the values of E_a^* were obtained.

In Figure 6 the values of ΔH^* obtained from the slope $\Delta H/2.303R$ while ΔS^* obtained from the intercepts are of log R/Nh + $\Delta S^*/2.303$ after we plot of log k_{corr} /T *versus* 1/T, which gives a straight line" [27].

The collected statistics are listed in (Table 4), and we understood from it that:

1. E_a^* values are higher in the presence of EA extract by comparison with the absence of EA due to the adsorption of the EA on CS surface and the formation of a thin protective layer which decreases CR. The values of E^*_a increase when EA concentration increases.

2. ΔS^* -ve sign illustrates that the activated complex at the rate-determining step prefers an association rather than a dissociation" [28].

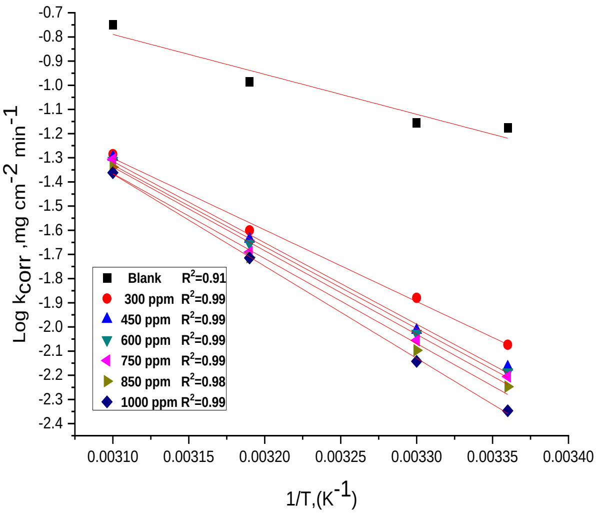

Figure 5. Plot of log k_{corr} vs. 1/ T for CS in the presence and absence of EA extract in 0.5M H_2SO_4.

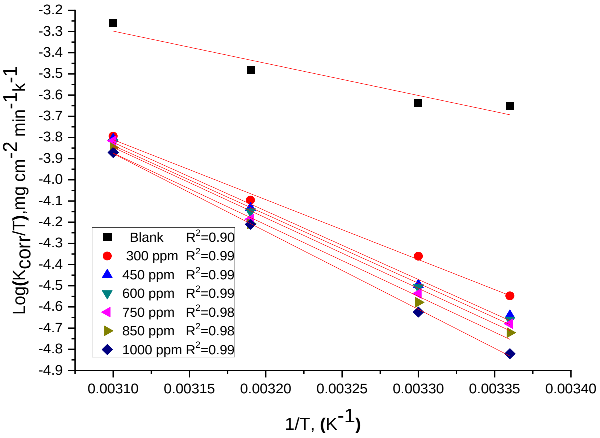

Figure 6. Plot of log k_{corr} / T vs 1/ T for CS in the presence and absence of EA extract in 0.5M H_2SO_4.

Table 4. Activation Parameters for CS in the presence and absence of EA extract in 0.5M H_2SO_4.

Conc, (ppm)	**E^*_a (kJ mol^{-1})**	**ΔH^* (kJ mol^{-1})**	**$-\Delta S^*$ (J mol^{-1}K^{-1})**
Blank	31.6	29.1	170
300	56.7	54.1	102
450	64.4	61.8	79
600	64.7	62.2	78
750	66.2	63.6	73
850	67.3	64.7	70
1000	72.9	70.3	53

3.2. EFM measurements.

Figure 7 illustrates the intermodulation spectra of CS in 0.5 M H_2SO_4 in the presence and absence of different concentrations of EA extract at 25°C. Table 5 shows the EFM findings (i_{corr}, β_c, β_a, CF-2, CF-3, and % IE). The results revealed that increasing the concentration of EA extract lowered i_{corr} while boosting inhibition efficiency (% IE). The found causality factors correspond to theoretical values.

Corrosion current densities are independent of the Tafel constant and may be estimated directly from EFM data. The % IE may be calculated using Eq.(12).

$$\%IE = 100 \times [1-(i_{corr}/i^o_{corr})] \qquad (12)$$

where i^{o}_{corr} and i_{corr} are corrosion currents in the absence and presence of EA extract, respectively.

The values of (CF-2 & CF-3) are quite similar to the theoretical values (2 & 3), indicating that the results are of high quality [29].

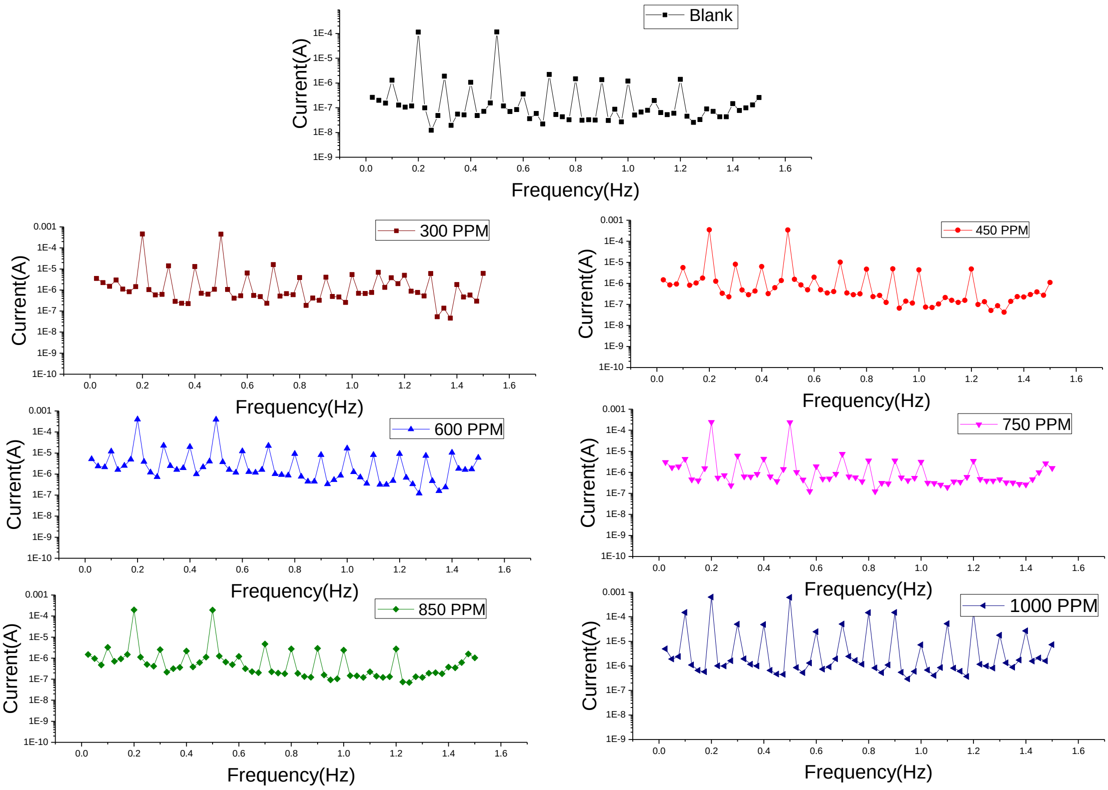

Figure 7. EFM data for CS in the presence and absence of different concs. of EA extracts.

Table 5. EFM data of CS corrosion at different concentrations of EA extract at 25°C.

[inh.] (ppm)	**i_{corr}, (μAcm^{-2})**	**β_c, (mVdec^{-1})**	**β_a, (mVdec^{-1})**	**CF-2**	**CF-3**	**Ө**	**%IE**
Blank	1006	68	162	2	3	--	--
300	235	64	177	2.1	2.7	0.766	76.6
450	205	61	188	2.4	2.4	0.796	79.6
600	209	71	166	1.9	2.3	0.792	79.2
750	157	64	154	1.9	2.9	0.844	84.4
850	133	66	159	1.9	2.7	0.868	86.8
1000	112	65	146	1.9	3.2	0.889	88.9

3.3. EIS method.

EIS is a helpful tool for investigating CS corrosion in the presence and absence of different concentrations of EA extract in 0.5M H_2SO_4. The Nyquist and Bode curves at the OCP at 25 °C are shown in Figures 8 and 9. At low frequencies, Nyquist plots are characterized by semicircle loops, which are illustrated easily in Figure 10 by the Randle circuit. This circuit depicts a parallel combination of a charge transfer resistance (R_{ct}) and a double layer capacitance (C_{dl}.), both in series with a solution resistance (R_s.) [30]. The associated R_{ct} was also used to compute IE and CPE, which are used to define the double layer [31]:

$$C_{dl} = Y_0 \,(2\pi f_{max})^{n-1} \qquad (13)$$

With $0 \leq n \leq 1$, $j = \sqrt{-1}$ and "f_{max} is the frequency of the highest imaginary value, Y_o is a frequency-independent constant, being defended as pure capacitance for n=1, resistance for n = 0, and inductance for n = -1. Diffusion processes are characterized by the value of n = 0.5. The divergence from optimal behavior is represented by the value of (n). The values of n, Y_0, R_{ct} charge transfer resistance, C_{dl} double layer capacitance, and %IE were obtained and recorded (Table 6). The Nyquist plots produced in the real system illustrate a generic behavior in which the double layer on the CS/solution interface does not act as a real capacitor. Table 6 displays the data gathered from the analogous circuit. The findings demonstrate that adding the inhibitor raised R_{ct} levels. This is because an insulating protective coating forms at the metal/solution interface. C_{dl} values were also reduced due to a drop in the local dielectric constant and/or an increase in the thickness of the electrical double layer, suggesting that the inhibitor molecules are adsorbed at the metal/solution interface [32]. Because EA molecules displace water molecules and are first adsorbed on the CS surface, their adsorption on the surface reduces electrical capacity.

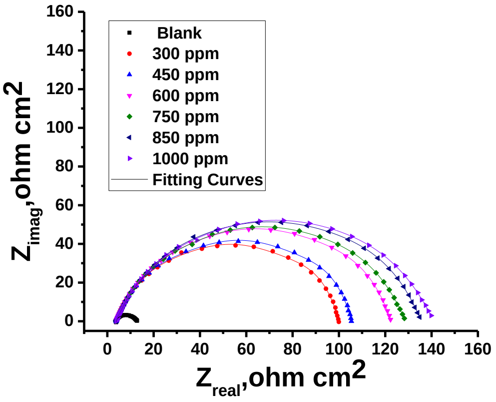

Figure 8. The Nyquist plots for CS in nonexistence and existence of various concentrations of EA extract at 25°C.

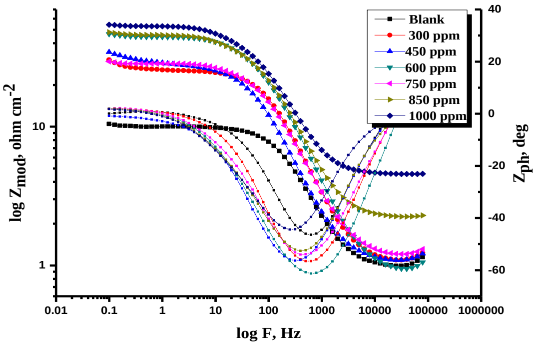

Figure 9. The Bode plots for the dissolution CS in nonexistence and existence of various concentrations of EA extract in 0.5M H2SO4 at25°C.

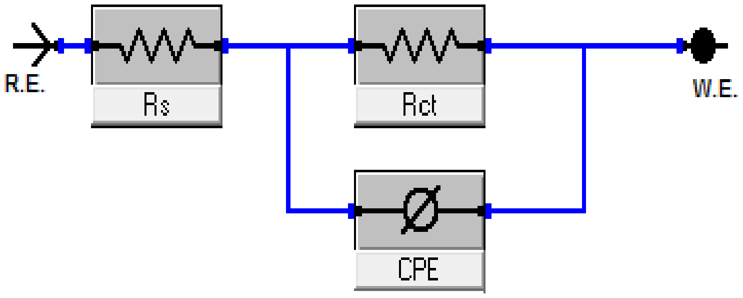

Figure 10. An equivalent circuit utilized to fit the EIS results.

Table 6. EIS value of CS in nonexistence and existence of various doses of EA extract at 25ºC.

[inh.] (ppm)	Y_o, ($\mu\ \Omega^{-1}\ s^n\ cm^{-2}$) x$10^{-6}$	R_{ct}, (Ω cm^{-2})	n	C_{dl}, ($\mu F cm^{-2}$)	θ	%IE
1 M HCl	503	9	0.843	184	--	--
50	131	78	0.848	60	0.885	88.5
100	130	104	0.847	59	0.913	91.3
150	129	120	0.843	56	0.925	92.5
200	128	126	0.822	52	0.929	92.9
250	126	133	0.818	50	0.932	93.2
300	122	137	0.814	48	0.934	93.4

3.4. PDP tests.

The influence of EA extract on the anodic & cathodic processes occurring in the system was studied using PDP measurements. At 25°C, Figure 11 depicts the potentiodynamic polarization curves for CS in the presence and absence of different concentrations of EA extract. Table 7 listed the electrochemical parameters Ecorr, β_a&β_c,θ, %IE, and i_{corr}. The results showed that adding EA extract reduced the corrosion current (icorr), decreased the CR, and increased the % IE owing to the establishment of a protective adsorbed layer of the plant extract. While the values of (E_{corr}) and (β_a&β_c) did not change considerably, the EA extract acted as a mixed inhibitor, inhibiting both the H_2 evolution (cathodic reaction) and the CS dissolving process (anodic reaction) [33-35]. Furthermore, the non-significant difference in β_a and β_c demonstrates that the EA extract does not influence the CS corrosion process in 0.5 M H_2SO_4. The (%IE) derived from icorr shows that the presence of different concentrations of EA extract reduces the anodic and cathodic current densities as well as the polarization resistance.

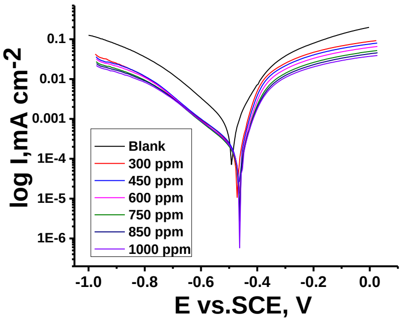

Figure 11. PP plots for the dissolution of CS in the presence and absence of various concentrations of EA extract.

Table 7. PP parameters of CS, including various concentrations of EA extract.

Conc., ppm	$i_{corr.}$ $\mu A\ cm^{-2}$	$-E_{corr.}$, mVvs SCE	β_a, mV dec^{-1}	β_c, mV dec^{-1}	C.R., mm y^{-1}	ϴ	% IE
Blank	997	490	62	183	380	-----	--
300	187	470	55	181	0.812	0.812	81.2
450	177	466	49	178	0.822	0.822	82.2
600	157	464	48	174	0.843	0.843	84.3
750	131	464	45	180	0.869	0.869	86.9
850	118	462	57	186	0.882	0.882	88.2
1000	88	462	63	190	0.912	0.912	91.2

3.5. Surface characterization.

3.5.1. AFM study.

The surface morphology of CS was studied by the AFM method while submerged in 0.5 M H_2SO_4 solution with & without 1000 ppm of EA extract and for pure CS samples following physical treatment as ML measurements. The 3-D picture of a pure CS surface (bare CS) with a clean and smooth surface is shown in Figure 12-a. The 3D picture of a CS surface in 0.5 M H_2SO_4 for 12 hours is shown in Figure 12-b. In this shot, the surface is noticeably eroded and degraded when contrasted to the clean surface of naked CS. The 3D picture for the CS surface was less corroded and smoother when 1000 ppm of the studied inhibitor was used, as shown in Figure 12-c. The 3-D picture for the CS surface was less corroded and smoother than the CS in 0.5 M H_2SO_4. Before and after adding the present inhibitor, the average roughness of the naked CS and CS surface in 0.5 M H_2SO_4 was 17.4 nm, 993.76 nm, and 122.8 nm, respectively. The findings and 3D pictures indicated that EA extract adsorption on the CS surface [36-39].

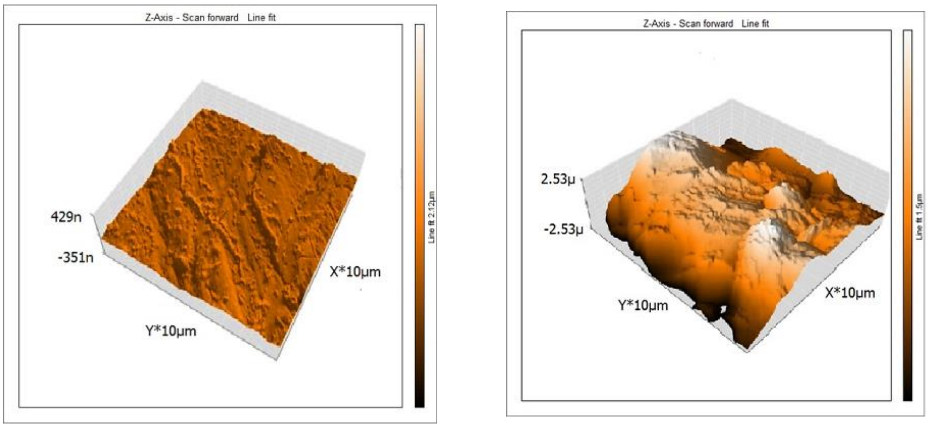

Free Blank

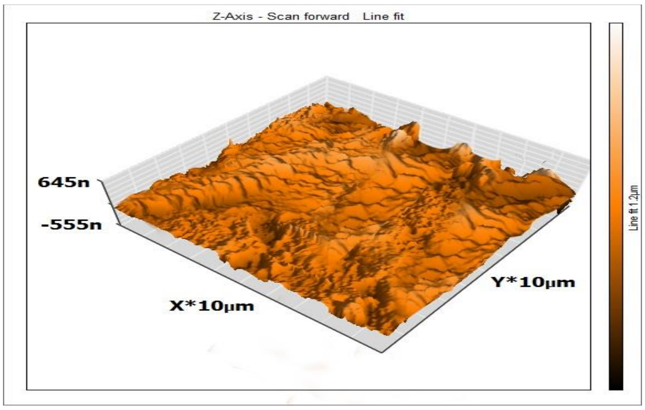

EA extract

Figure 12. AFM 2D (free), 3D (Blank) of CS free surface, and 3D (EA extract). Note: Free and blank samples (Fig.12 a,b) were taken from the paper reference [40].Same CS sample composition, same time of immersion (12 h), 0.5 M H_2SO_4, and same corresponding author

3.5.2. XPS.

The protective layer formed on the CS surface in 0.5M H_2SO_4, as well as proving the adsorption nature of the EA extract. Figure 13 shows the XPS decomposition spectra for each element separately, which are found in the surface layer formed in a solution that controls the presence of the composition of the EA extract. The CS metal spectra recorded when immersed in a 0.5M H_2SO_4 containing the highest concentration of EA extract (1000 ppm) were for Cl 2p, Fe 2p, O 1s, N1s, and C1s. Table 8 shows the binding energies date(BE, eV) and the same assignment for every peak component [41,42]. Different peaks were observed at binding energy values of the Cl 2p, Fe 2p, O 1s, N1s, and C1s, found in 0.5M Sulfuric acid and 1000 ppm of EA extract. Previous results obtained from XPS analysis confirmed the adsorption of EA molecules on the CS surface.

Survey

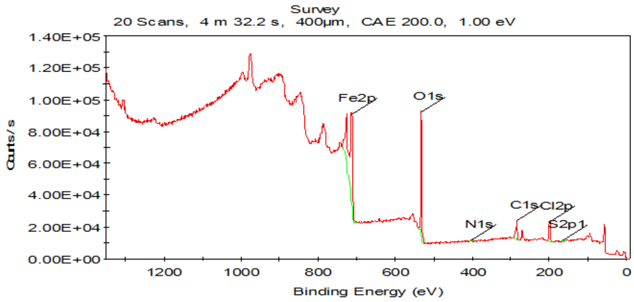

Fe2p

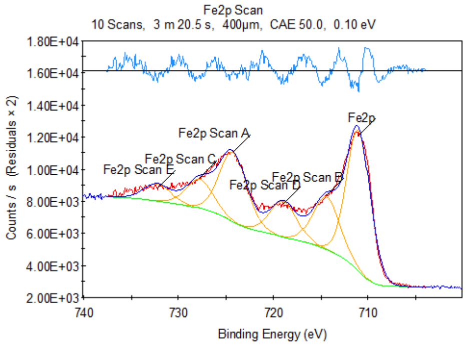

O1s

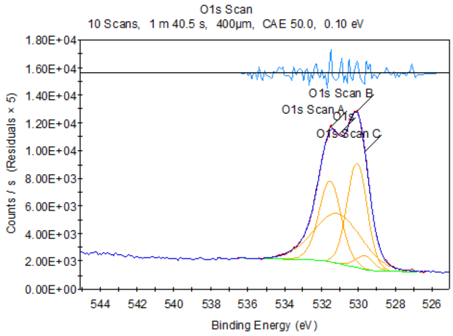

N1s

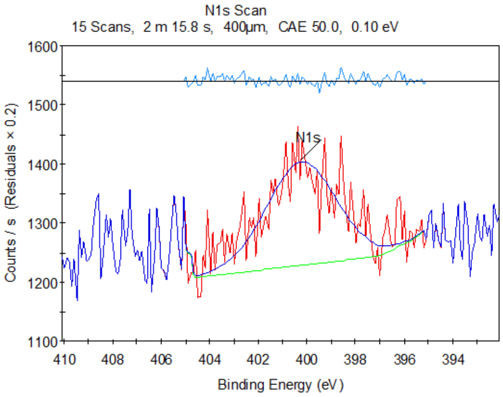

C1s

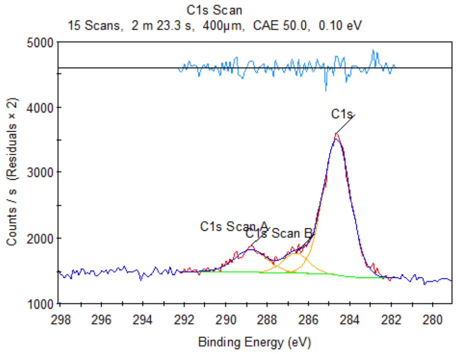

Cl2p

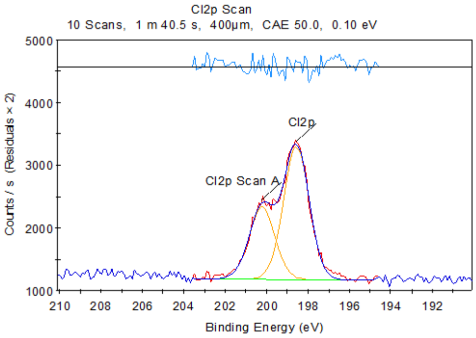

S2p1

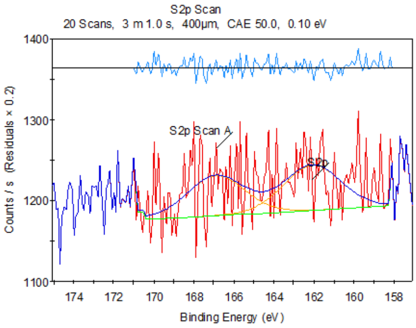

Figure 13. Photoelectric X-rays results from Survey, Fe2p, O 1s, N1s, C1s, and Cl2p for Cs at 0.5M sulfuric acid solutions with 1000 ppm from *Erica arborea* extract.

Table 8. The determination of binding energies (eV) for the large core lines noticed for the surface of Csl, which handled by *Erica arborea* extract

Core element	BE, eV	Assignments
C1s	292.17	C-C, -C=O,C-H
	286.91	
	288.34	
O1s	521.87	Fe_2O_3 , $Fe(OH)_3$
	536.18	
N1s	401.03	N-Fe
Fe2p	710.59	Fe_2O_3/ Fe_3O_4/ FeOOH $FeCl_3$
	721.07	
	718.34	
	714.41	
	728.99	
Cl2p	198.8	Cl 2p3/2
S2p1	165.1	S-Fe

4. Mechanism of Corrosion Inhibition

Mass loss and electrochemical studies show that using EA extract reduces CS deterioration. The results demonstrated that the inhibition mechanism depends on the adsorption of EA extract to active areas on the CS surface. Aside from the availability of π electrons in the aromatic system, the adsorption of EA extract is carried out by the adsorption of heteroatoms of the inhibitor that are present in various ingredients of the extract [43,44]. We know from phytochemical studies that EA extract has a wide range of organic substances. The findings of the temperature investigation revealed that mechanical adsorption occurs via physical adsorption. Because of its +ve charge, the CS surface favors SO_4^{-2} adsorption to generate a -ve charge surface. Therefore, this chemical (EA extract) will be present. Because these molecules (EA extract) are protonated, they may adsorb directly on the negative surface of CS [45,46] in an acidic solution via electrostatic attraction, as illustrated in Figure 14.

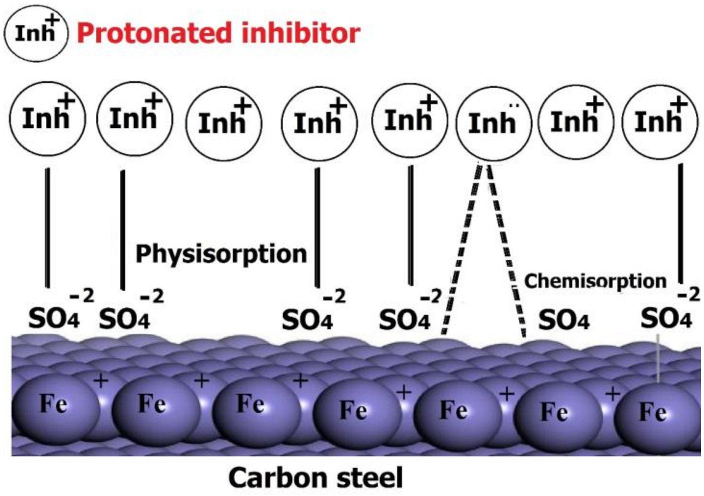

Figure 14. Mechanism of corrosion inhibition of EA extract.

5. Conclusions

The following conclusions are based on the preceding findings: EA extract is a useful inhibitor used to constrict the corrosion of CS in H_2SO_4 solutions; The results data revealed that raising the concentration of EA extract increased the inhibitory efficiency (%IE);

Regardless of the blank solution, when the EA extract is introduced, the double-layer capacitances decrease, and the charge transfer resistance increases; EA extract adsorption follows the Langmuir adsorption isotherm; The findings revealed that the EA extract acts as a mixed-type inhibitor; The techniques utilized to identify the corrosion inhibition process, Ml, PDP, EFM, and EIS, are rather well agreed upon; Chemical and electrochemical procedures are very compatible.

Funding

This research received no external funding.

Acknowledgments

We are grateful to the unknown referees for the attentive reading of the article and insightful comments that aided in creating this research into its current form. We want to express our gratitude to the corrosion chemistry laboratory team at Mansoura University (Egypt) for their appreciative and respectful cooperation.

Conflicts of Interest

The authors declare no conflict of interest.

References

1. Nazeera Banu, V.R.; Rajendran S.; Senthil Kumaran S. Investigation of the inhibitive effect of Tween 20 self assembling nanofilms on corrosion of carbon steel. *J. Alloys Compd.* **2016**, *675*, 139-148, https://doi.org/10.1016/j.jallcom.2016.02.247.
2. Chauhan, L. R.; Gunasekaran G. Corrosion inhibition of mild steel by plant extract in dilute HCI medium. *Corrosion Sci.* **2007**, *49*, 1143-61, https://doi.org/10.1016/j.corsci.2006.08.012.
3. Lalitha, A.; Ramesh, S.; Rajeswari, S. Surface protection of copper in acid medium by azoles and surfactants. *Electrochim. Acta.* **2005**, *51*, 47-55, https://doi.org/10.1010j.electacta.2005.04.003.
4. Quraishi, M. A.; Sardar, R. Dithiazolidines - a new class of heterocyclic inhibitors for prevention of mild steel corrosion in hydrochloric acid solution. *Corrosion* **2002**, *58*, 103-7, https://doi.org/10.5006/1.3277308.
5. Abdel-Rehim, S.S.; Khaled, K. F.; Abd-Elshafi, N.S. Electrochemical frequency modulation as a new technique for monitoring corrosion inhibition of iron in acid media by new thiourea derivative. *Electrochim. Acta.* **2006**, *51*, 3269-77, https://doi.org/10.1016/j.electacta.2005.09.018.
6. Zaher, A.; Aslam, R.; Lee, H.S.; Khafouri, A.; Boufellous, M.; Alrashdi, A.A.; Lgaz, H.; Ouhssine, M. A combined computational & electrochemical exploration of the Ammi visnaga L. extract as a green corrosion inhibitor for carbon steel in HCl solution. *Arabian Journal of Chemistry*. **2022**, *15*, 103573, https://doi.org/10.1016/j.arabjc.2021.103573.
7. Fouda, A.S.; Motaal, S.M.A.; Ahmed, A.S.; Sallam, H.B.; Ezzat, A.; El-Hossiany, A. Corrosion Protection of Carbon Steel in 2M HCl Using Aizoon canariense Extract. *Biointerface Res. Appl. Chem*. **2022,** *12*, 230-249, https://doi.org/10.33263/BRIAC121.230243.
8. Verma, C.; Ebenso, E.E.; Bahadur, I.; Quraishi, M.A. An overview on plant extracts as environmental sustainable and green corrosion inhibitors for metals and alloys in aggressive corrosive media. *J. Mol. Liq.* **2018**, 266, 577–590, https://doi.org/10.1016/j.molliq.2018.06.110.
9. Harb, M.B.; Abubshait, S.; Etteyeb, N.; Kamoun, M.; Dhouib, A. Olive leaf extract as a green corrosion inhibitor of reinforced concrete contaminated with seawater. *Arabian J. Chem.* **2020**, *13*, 4846–4856, https://doi.org/10.1016/j.arabjc.2020.01.016.
10. Ikpeseni, S.C.; Odu, G.O.; Owamah, H. I.; Onochie, P.U.; Ukala, D. C. Thermodynamic parameters and adsorption mechanism of corrosion inhibition in mild steel using jatropha leaf extract in hydrochloric acid. *Arabian Journal for Science and Engineering*. **2021**, *2021*, 1–11, https://doi.org/10.1007/s13369-021-05488-9.
11. Kouache, A.; Khelifa, A.; Boutoumi, H.; Moulay, S.; Feghoul, A.; Idir, B.; Aoudj, S. Experimental and theoretical studies of Inula viscosa extract as a novel eco-friendly corrosion inhibitor for carbon steel in 1 M HCl. *Journal of Adhesion Science and Technology*. **2022,** *36*, 988-1016, https://doi.org/10.1080/01694243.2021.1956215.

12. Vuong, B.X.; Huynh, T.L.; Tran, T.Q.N.; Vattikuti, S.P.; Manh, T.D.; Nguyen-Tri, P.; Nguyen, A.T.; Van Hien, P.; Dang, N.N. Corrosion inhibition of carbon steel in hydrochloric acid solution by self-formation of a Malpighia glabra leaf extract-based organic film. *Materials Today Communications*. **2022,** *31,* 103641, https://doi.org/10.1016/j.mtcomm.2022.103641.
13. Sannaiah, P.N.; Alva, V.D.P.; Bangera, S. An experimental, theoretical, and spectral approach to evaluating the effect of eco-friendly Oxalis stricta leaf extract on the corrosion inhibition of mild steel in 1 N H2SO4 medium. *Journal of the Iranian Chemical Society*. **2022,** *19,* 1817-1835, https://doi.org/10.1007/s13738-021-02422-6.
14. Wan, S.; Wei, H.; Quan, R.; Luo, Z.; Wang, H.; Liao, B.; Guo, X. Soybean extract firstly used as a green corrosion inhibitor with high efficacy and yield for carbon steel in acidic medium. *Industrial Crops and Products*. **2022**, *1,* 115354, https://doi.org/10.1016/j.indcrop.2022.115354.
15. Hossain, N.; Chowdhury, M.A.; Rana, M.; Hassan, M.; Islam, S. Terminalia arjuna leaves extract as green corrosion inhibitor for mild steel in HCl solution. *Results in Engineering*. **2022**, *11,* 100438, https://doi.org/10.1016/j.rineng.2022.100438.
16. Bessah, R.; Benyoussef, E. H. Essential oil composition of *Erica arborea* L. leaves from Algeria. *Journal of Essential Oil Bearing Plants* **2014**, *17,* 931-935, https://doi.org/10.1080/0972060X.2014.895184.
17. Zengin, G.; Cvetanović, A.; Gašić, U.; Stupar, A.,; Bulut, G.; Senkardes, I.; Dogan, A.; Seebaluck-Sandoram, R.; Rengasamy, K. R.; Sinan, K.I.; Mahomoodally, M.F. Chemical composition and bio-functional perspectives of *Erica arborea* L. extracts obtained by different extraction techniques: Innovative insights. *Industrial Crops and Products* **2019**, *142*, 111843, https://doi.org/10.1016/j.indcrop.2019.111843.
18. Khaled, M.A.; Ismail, M.A.; El-Hossiany, A.A.; Fouda, A.S. Novel pyrimidine-bichalcophene derivatives as corrosion inhibitors for copper in 1 M nitric acid solution. *RSC Advances* **2021**, *11*, 25314-25333, https://doi.org/10.1039/D1RA03603C.
19. Núñez-Morales, J.; Jaramillo, L. I.; Espinoza-, P. J.; Sánchez-Moreno, V. E. Evaluation of Adding Natural Gum to Pectin Extracted from Ecuadorian Citrus Peels as an Eco-Friendly Corrosion Inhibitor for Carbon Steel. *Molecules* **2022**, *27*,2111, https://doi.org/10.3390/molecules27072111.
20. Fouda, A.S.; Badr, S.E.; Ahmed, A.M.; El-Hossiany, A. Chemical and electrochemical corrosion of a copper alloy in aqueous solutions by using morus alba extract as an eco-friendly inhibitor, *Int. J. Corros. Scale Inhib.* **2021**, *10,* 1011–1029, https://doi.org/10.17675/2305-6894-2021-10-3-12.
21. Khadraoui, A.; Khelifa, A.; Hamitouche, H.; Mehdaoui, R. Inhibitive effect by extract of Mentha rotundifolia leaves on the corrosion of steel in 1 M HCl solution. *Research on Chemical Intermediates* **2014**, *40,* 961-972, https://doi.org/10.1007/s11164-012-1014-y.
22. Amira, E.; Seham, M. A.; Amal S. A.; Hayanem B. S.; El-Hossiany, A.; Fouda, A. S. Corrosion Inhibition of Carbon Steel in 2.0M HCl Solution Using Novel Extract (Pulicaria undulate), *Biointerface Res. Appl. Chem*. **2022**, *12*, 6415-6427, https://doi.org/10.33263/BRIAC125.64156427.
23. Prifiharni, S.; Mashanafie, G.; Priyotomo, G.; Royani, A.; Ridhova, A.; Elya, B.; Soedarsono, J. W. Extract sarampa wood (Xylocarpus Moluccensis) as an eco-friendly corrosion inhibitor for mild steel in HCl 1M. *Journal of the Indian Chemical Society*. **2022**, *99,*100520, https://doi.org/10.1016/j.jics.2022.100520.
24. Kumar, H.; Yadav, V.; Kumari, A. Adsorption, corrosion inhibition mechanism, and computational studies of Azadirachta indica extract for protecting mild steel: Sustainable and green approach. *Journal of Physics and Chemistry of Solids.* **2022**, *165*, 110690, https://doi.org/10.1016/j.jpcs.2022.110690.
25. Zaher, A.; Aslam, R.; Lee, H. S.; Khafouri, A.; Boufellous, M.; Alrashdi, A. A.; Lgaz, H.; Ouhssine, M. A combined computational & electrochemical exploration of the Ammi visnaga L. extract as a green corrosion inhibitor for carbon steel in HCl solution. *Arabian Journal of Chemistry*, **2022**, *15*, 103573, https://doi.org/10.1016/j.arabjc.2021.103573.
26. Boumhara, K.; Harhar, H.; Tabyaoui, M.; Bellaouchou, A.; Guenbour, A.; Zarrouk, A. Corrosion Inhibition of Mild Steel in 0.5 M H_2SO_4 Solution by Artemisia herba-alba Oil. *Journal of Bio- and Tribo-Corrosion* **2018**, 1-5, https://doi.org/10.1007/s40735-018-0202-8.
27. Feng, L.; Zhang, S.; Hao, L.; Du, H.; Pan, R.; Huang, G.; Liu, H. Cucumber (Cucumis sativus L.) Leaf Extract as a Green Corrosion Inhibitor for Carbon Steel in Acidic Solution: Electrochemical, Functional and Molecular Analysis. *Molecules* **2022**, *27*, 3826, https://doi.org/10.3390/molecules27123826.
28. Fouda, A.S.; Abdel Azeem, M.; Mohamed, S.A., El-Hossiany, A.; El-Desouky, E. Corrosion Inhibition and Adsorption Behavior of Nerium Oleander Extract on Carbon Steel in Hydrochloric Acid Solution. *Int. J. Electrochem. Sci*. **2019,** *14*, 3932 – 3948, https://doi.org/10.20964/2019.04.44.
29. Fouda, A.S.; Rashwan, S.; El-Hossiany, A.; El-Morsy, F. E. Corrosion Inhibition of Zinc in Hydrochloric Acid Solution using some organic compounds as Eco-friendly Inhibitors. *JCBPS.* **2019,** *9*, 001-024, https://doi.org/10.24214/jcbps.A.9.1.00124.
30. Kouache, A.; Khelifa, A.; Boutoumi, H.; Moulay, S.; Feghoul, A.; Idir, B.; Aoudj, S. Experimental and theoretical studies of Inula viscosa extract as a novel eco-friendly corrosion inhibitor for carbon steel in 1 M HCl. Journal of Adhesion Science and Technology. **2022**, *36*, 988-1016, https://doi.org/10.1080/01694243.2021.1956215.

31. Batah, A.; Chaouiki, A.; El Mouden, O.I.; Belkhaouda, M. H.; Bammou, L.; Salghi, R. Almond waste extract as an efficient organic compound for corrosion inhibition of carbon steel (C38) in HCl solution. *Sustainable Chemistry and Pharmacy* **2022**, *27*, 100677, https://doi.org/10.1016/j.scp.2022.100677.
32. Boukhedena, W.; Deghboudj, S.; Benahmed, M.; Laouer H. Experimental Study and Modeling of the Corrosion Inhibition of Mild Steel in 1M Hcl with Novel Friendly Butanolic Extract of Ephedra Major. *Journal of the Mexican Chemical Society*. **2022**, *66*, https://doi.org/10.29356/jmcs.v66i2.1630.
33. Soltani, N.; Tavakkoli, N.; Attaran, A.; Karimi, B.; Khayatkashani, M. Inhibitory effect of Pistacia khinjuk aerial part extract for carbon steel corrosion in sulfuric acid and hydrochloric acid solutions. *Chemical Papers* **2020**, *74*, 1799-1815, https://doi.org/10.1007/s11696-019-01026-y.
34. Abdelaziz, S.; Benamira, M.; Messaadia, L.; Boughoues, Y.; Lahmar, H.; Boudjerda, A. Green corrosion inhibition of mild steel in HCl medium using leaves extract of Arbutus unedo L. plant: An experimental and computational approach. *Colloids and Surfaces A: Physicochemical and Engineering Aspects* **2021**, *619*, 126496, https://doi.org/10.1016/j.colsurfa.2021.126496.
35. Elgyar, O.A.; Ouf, A.M.; El-Hossiany, A.; Fouda, A.S. The inhibition action of viscum album extract on the corrosion of carbon steel in hydrochloric acid solution. *Biointerface Res. Appl. Chem*. ***2021,*** *11*, 14344-14358, https://doi.org/10.33263/BRIAC116.1434414358.
36. Vuong, B. X.; Huynh, T. L.; Tran, T. Q.; Vattikuti, S. P.; Manh, T. D.; Nguyen-Tri, P.; Nguyen, A. T.; Van Hien, P.; Dang, N. N. Corrosion inhibition of carbon steel in hydrochloric acid solution by self-formation of a Malpighia glabra leaf extract-based organic film. *Materials Today Communications* **2022**, *31*,103641, https://doi.org/10.1016/j.mtcomm.2022.103641.
37. Fouda, A. S.; Ahmed, R. E.; El-Hossiany, A. Chemical, electrochemical and quantum chemical studies for famotidine drug as a safe corrosion inhibitor for α-brass in HCl solution. *Protection of Metals and Physical Chemistry of Surfaces* **2021**, *57*, 398-411, https://doi.org/10.1134/S207020512101010X.
38. Hsissou, R.; Abbout, S.; Berisha, A.; Berradi, M.; Assouag, M.; Hajjaji, N.; Elharfi, A. Experimental, DFT and molecular dynamics simulation on the inhibition performance of the DGDCBA epoxy polymer against the corrosion of the E24 carbon steel in 1.0 M HCl solution. *Journal of Molecular Structure* **2019**, *1182*, 340-351, https://doi.org/10.1016/j.molstruc.2018.12.030.
39. Fouda, A.S.; El-Gharkawy, E.S.; Ramadan, H.; El-Hossiany, A. Corrosion resistance of mild steel in hydrochloric acid solutions by clinopodium acinos as a green inhibitor. *Biointerface Res. Appl. Chem*. ***2021,*** *11*, 9786, https://doi.org/10.33263/BRIAC112.97869803.
40. Fouda A.S., Shalabi K., Alsadeag A., Inhibitive effect of artemisia judaica extract as green corrosion inhibitor for carbon steel in sulfuric acid solution, *Int J Petrochem Sci Eng.* **2017**, *2(7)*, 228–236.
41. Manh, T.D.; Huynh, T.L.; Thi, B. V.; Lee, S.; Yi, J.; Nguyen Dang, N. Corrosion Inhibition of Mild Steel in Hydrochloric Acid Environments Containing Sonneratia caseolaris Leaf Extract. *ACS omega*. **2022**, *7*, 8874-86, https://doi.org/10.1021/acsomega.1c07237.
42. Rani, A.T.; Thomas, A,.; Williams, L.; Joseph, A. Effect of Lunamarine, the Major Constituent of Boerhaavia diffusa Leave Extract on the Corrosion Inhibition of Mild Steel in Hydrochloric Acid; Computational Modelling, Surface Screening and Electroanalytical Studies. *Journal of Bio-and Tribo-Corrosion*. **2022**, *8*, 1-21, https://doi.org/10.1007/s40735-021-00616-2.
43. Wang, Q.; Zhang, Q.; Liu, L.; Zheng, H.; Wu, X.; Li, Z.; Gao, P.; Sun, Y.; Yan, Z,.; Li, X. Experimental, DFT and MD evaluation of Nandina domestica Thunb. extract as green inhibitor for carbon steel corrosion in acidic medium. Journal of *Molecular Structure.* 2022, *24*, 133367, https://doi.org/10.1016/j.molstruc.2022.133367.
44. Fouda, A.S.; Abdel-Latif, E.; Helal, H. M.; El-Hossiany, A. Synthesis and characterization of some novel thiazole derivatives and their applications as corrosion inhibitors for zinc in 1 M hydrochloric acid solution. *Russian Journal of Electrochemistry*. **2021**, *57*, 159-71, https://doi.org/10.1134/S1023193521020105.
45. Ali, M.A.; Ouf, A.M.; El-Hossiany, A.; Fouda, A.S. Eco-friendly approach to corrosion inhibition of copper in hno3 solution by the expired tylosin drug. *Biointerface Res. Appl. Chem.* **2022**, *12*, 5116-30, https://doi.org/10.33263/BRIAC124.51165130.
46. Khadom, A. A.; Jassim, S. A.; Kadhim, M.M.; Ali, N. B. Influence of apricot constituents as eco-friendly corrosion inhibitor for mild steel in acidic medium: A theoretical approach. *Journal of Molecular Liquids*. **2022**, *347*, 117984, https://doi.org/10.1016/j.molliq.2021.117984.